SUPPORTING INFORMATION

Simultaneous Binding of Folic Acid and Methotrexate to Human Serum Albumin: Insights into the Structural Changes of Protein, and the Location and Competitive Displacement of Drugs

Sudipta Panja, Deb Kumar Khatua, and Mintu Halder*

Department of Chemistry, Indian Institute of Technology Kharagpur

Kharagpur-721302, India

*Corresponding author: mintu@chem.iitkgp.ernet.in

Phone: +91-3222-283314, FAX: +91-3222-282252

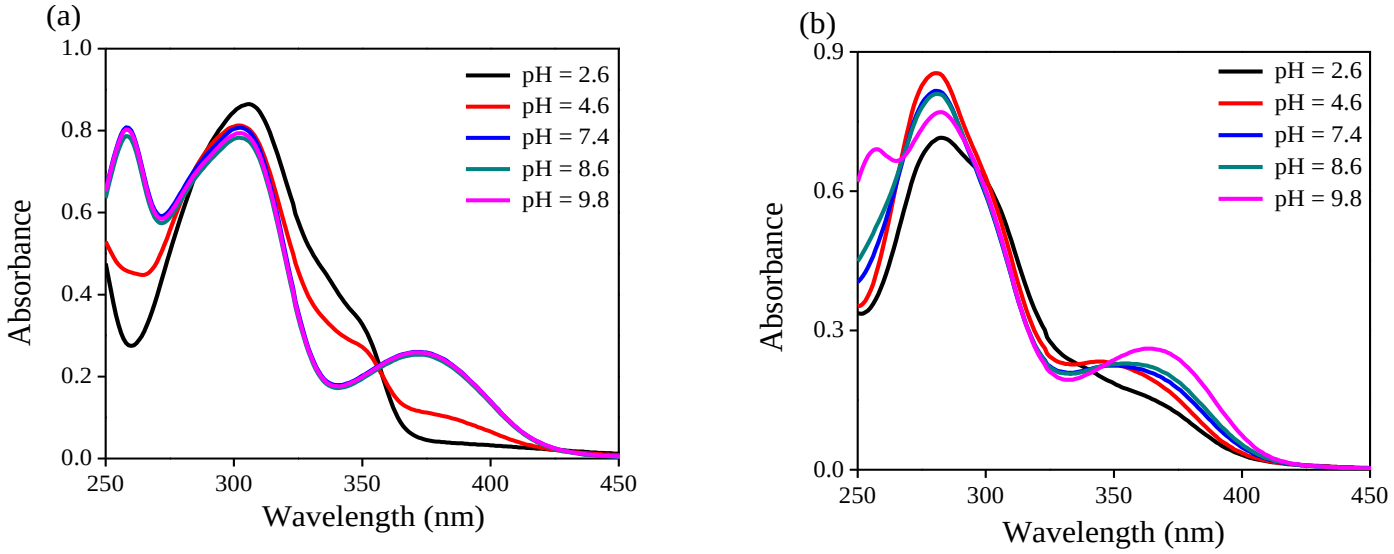

Figure S1. Absorption spectra of (a) MTX (30 μM) and (b) FA (30 μM) at several pH conditions

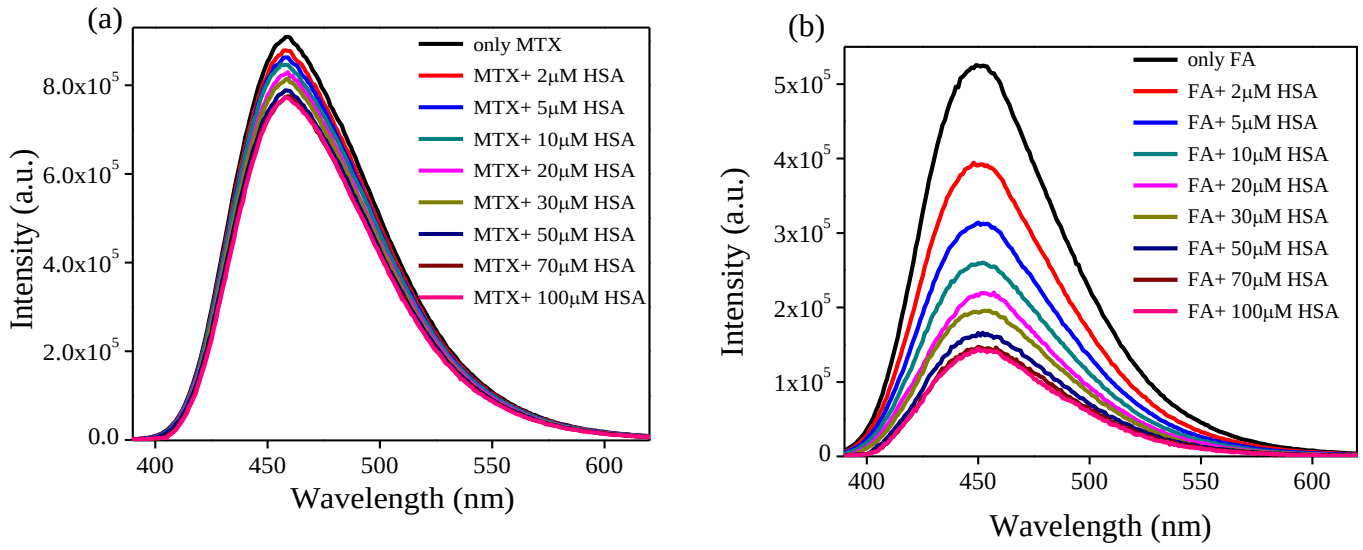

Figure S2. Corrected emission spectrum of (a) MTX (10 μM) and (b) FA (10 μM) in absence and presence of HSA at pH 7.4.

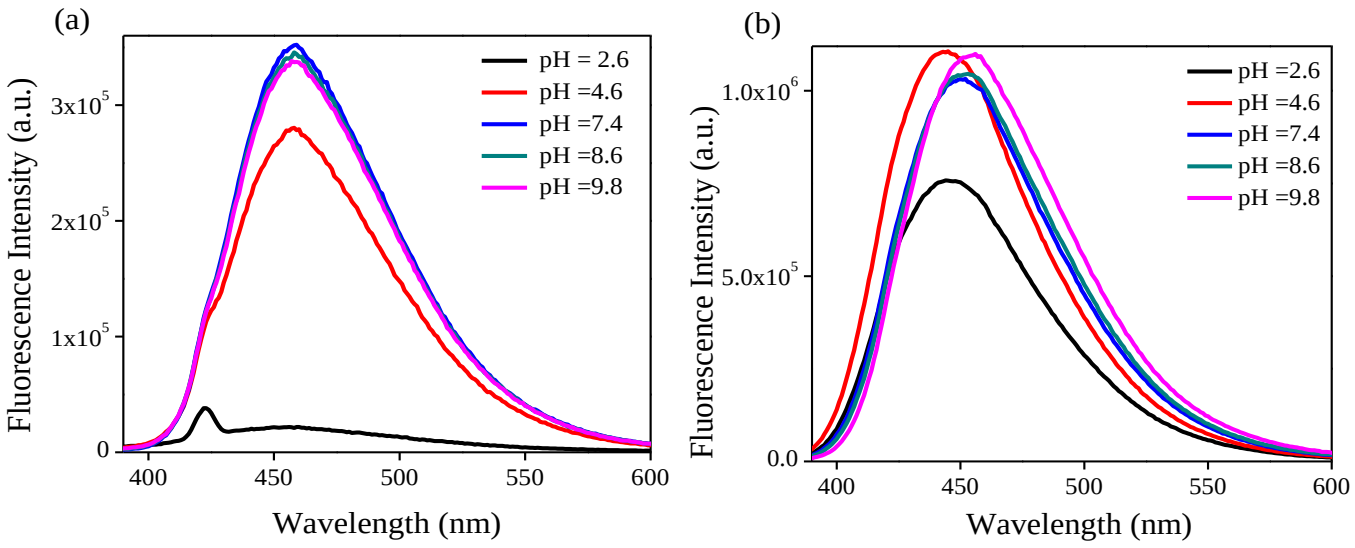

Figure S3. Fluorescence spectra of (a) MTX (10μM) and (b) FA (10μM) at different pH values.

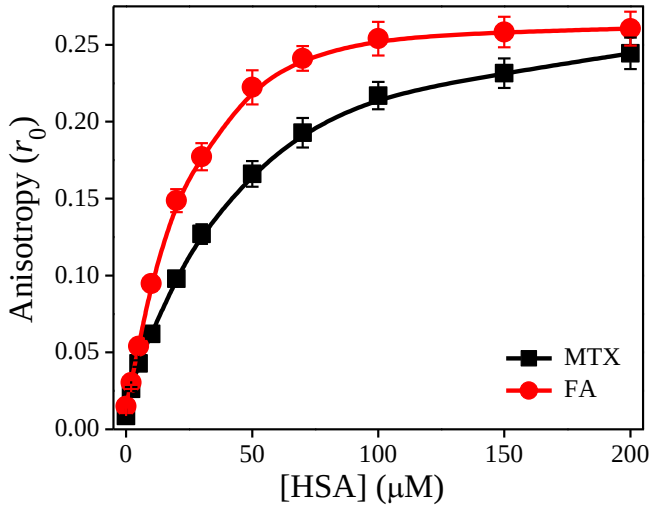

Figure S4. Change of steady-state fluorescence anisotropy of MTX (10μM) and FA (10μM) with increasing concentration of HSA (0 to 100μM).

Time Resolved Fluorescence Studies

Fluorescence decay measurement

In order to interpret the dynamics of the drug molecule within the heterogeneous environment, the time-resolved fluorescence decay of MTX and FA has been recorded in the presence of HSA. Representative decay profiles are highlighted in Figure S5 and fitted data are tabulated in Table S1. The time-resolved fluorescence decay of MTX and FA in aqueous buffer (Phosphate buffer, pH 7.4) is found to exhibit a bi-exponential and tri-exponential decay function, respectively. The decay MTX consists of two lifetime components of 2.27 ns (81%) and 6.95 ns (19%), which correspond to the neutral form. In case of FA, faster decay component (0.53 ns) is having the major contribution (77%) and two slow decaying components have the rest of the contribution (2.85 ns having 13% contribution and 7.39 ns having 10% contribution). In physiological pH condition the FA mostly assumes in the neutral form (pK_a ~ 8.38). Tabulated data (Table 1) infers that with increasing protein concentration, the lifetime of the 2.27

ns component of MTX shows minimal change (from 2.27 ns to 2.25 ns with increasing concentration of HSA from 0 to 100 μM), but shows a substantial decrease in amplitude (from 0.81 to 0.34) and this is accompanied by the appearance of a new fast decaying component (~460 ps). This new component could arise due to the formation of MTX-HSA complex and shorter lifetime value signifies possible energy transfer between MTX and side chain residues of the protein. Now the unbound form FA shows three lifetime components and with increasing protein concentration the two fast components are affected similar way as happened with MTX, which leads to decrease of the average lifetime value (1.52 ns -1.09 ns). A similar decrease of τ_{avg} from 3.16 ns to 2.10 ns is also observed for MTX. As seen in Table 1, the τ_{avg} of the drugs drops down progressively with increasing HSA, so from here we can estimate the distribution of radiative (k_r) and non-radiative (k_{nr}) decay rate constants of the drug in the aqueous buffer and HSA according to the following equations:[1]

$$\kappa_r = \frac{\Phi}{\tau_{avg}} \quad \text{.....(S1)}$$

$$\kappa_{nr} = \frac{1}{\tau_{avg}} - \kappa_r \quad \text{.....(S2)}$$

The changes in value of the of quantum yield (Φ), τ_{avg} , k_r and k_{nr} are summarized in Table 1, which infers that with increasing concentration of HSA the radiative decay rates are not sufficiently perturbed (infact k_r decreases in case of FA and slightly increases in case of MTX) and makes this process less important to nonradiative process. Because, with addition of HSA the nonradiative channel are greatly enhanced and makes more impact on average lifetime values. So τ_{avg} values are mainly attributed the nonradiative decay process and it depends upon the location of drug molecule in micro-heterogeneous protein pocket. After all the protein side chain residue also impart significant role in the binding process through the formation of rigid protein drug complex and facilitate the possibility of electron transfer between them

and also anticipate the very short life time intra molecular electron transfer process from the 4-aminobenzoyl to pterin ring of FA.[2]

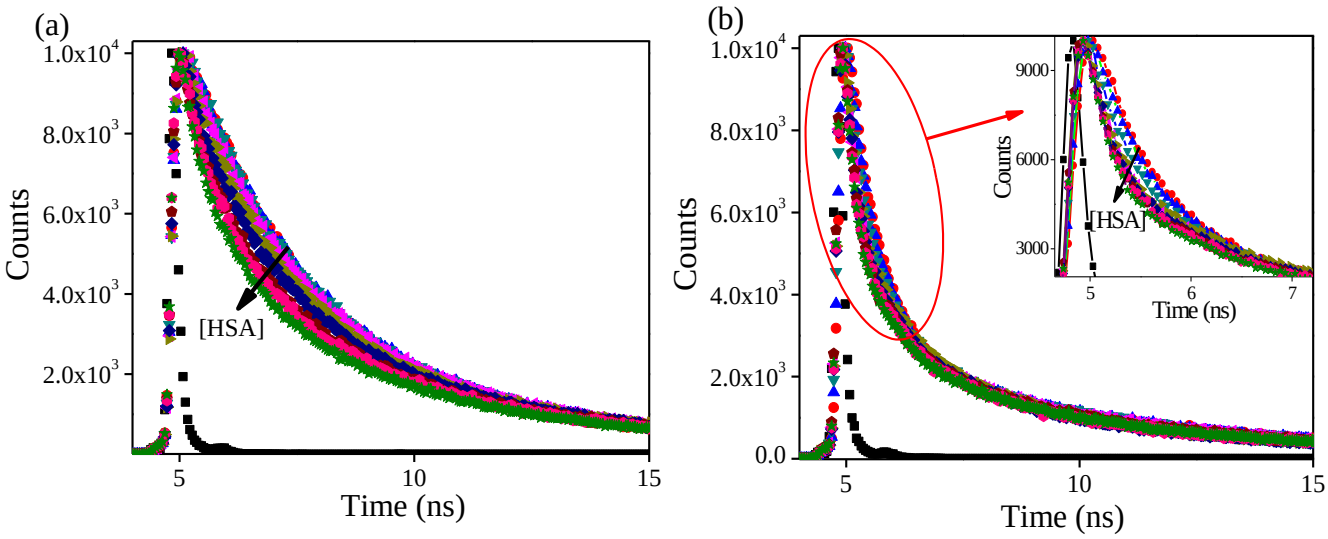

Figure S5. Fluorescence decay profile of (a) MTX (10μM) and (b) FA (10μM) in absence and presence of HSA at 298K.

Fluorescence anisotropy decay measurement

The time resolved anisotropy measurements provide information about the alteration of microenvironment around the drug molecule.[1] The estimated rotational correlation time (τ_r) also furnishes the extent of rigidity of any microheterogeneous media.[1] Therefore, the time-resolved anisotropy measurement provides additional information about the bound and unbound forms of the drug in protein drug complexation. The typical anisotropy decay profiles of the drug in the aqueous buffer as well as in the protein environment are highlighted in Figure S6 and the fitted data are summarized in Table S2. In aqueous buffer medium both of the drug exhibit single rotational decay time (0.20 ns for MTX and 0.11 for FA), indicate that unbound (free) form of the drugs is experiencing a homogeneous medium. In

protein environment, biexponential anisotropy decay is observed for FA, which is due to the presence of bound and unbound forms. The bound form localizes strongly in protein pocket makes the rotational decay time much slower and the faster motion is attributed to the solvent exposed form of the drug molecule. Whereas in the proteinous medium MTX exhibit only single exponential decay and the rotational time increases with addition of HSA, indicate that in protein medium MTX experience almost same surroundings. Moreover, in this microheterogeneous medium, the average rotational time (θ_r) of FA (2.28 ns) is much higher than that for MTX (1.34 ns), due to a larger contribution of slow rotational species (5.39 ns), regarded as the bound form. Therefore, FA binds with HSA maintaining the simultaneous equilibrium between two forms and as the anionic form has grater binding ability than neutral form towards HSA, and this could be the possible cause of higher value of rotational time of the FA over MTX.

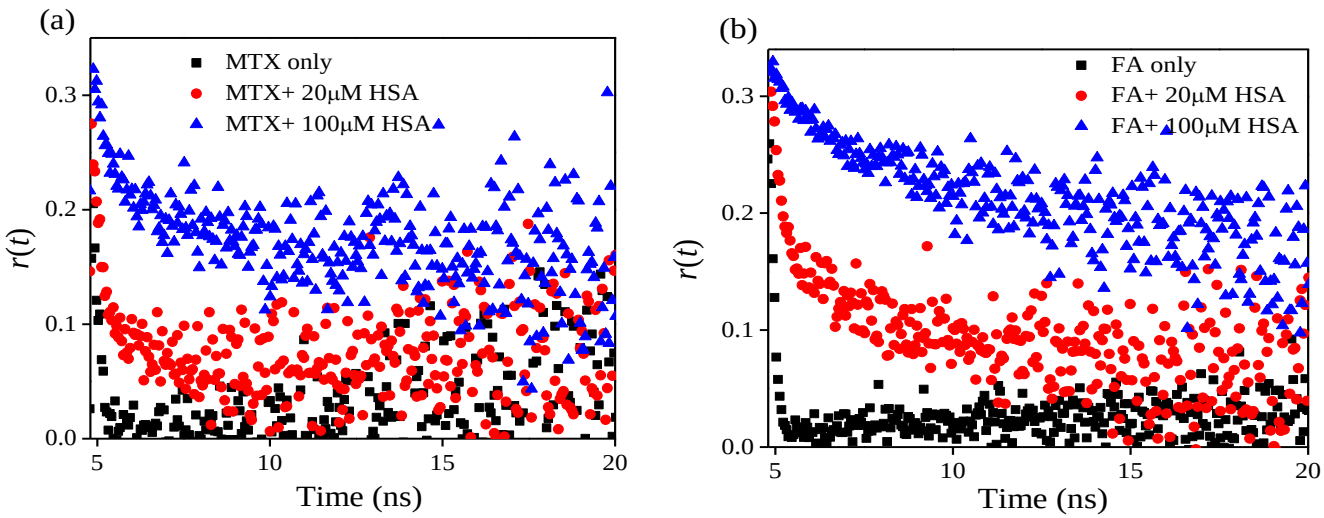

Figure S6. Change in time resolved fluorescence anisotropy of (a) MTX (10μM) and (b) FA (10μM) with increasing concentration of HSA.

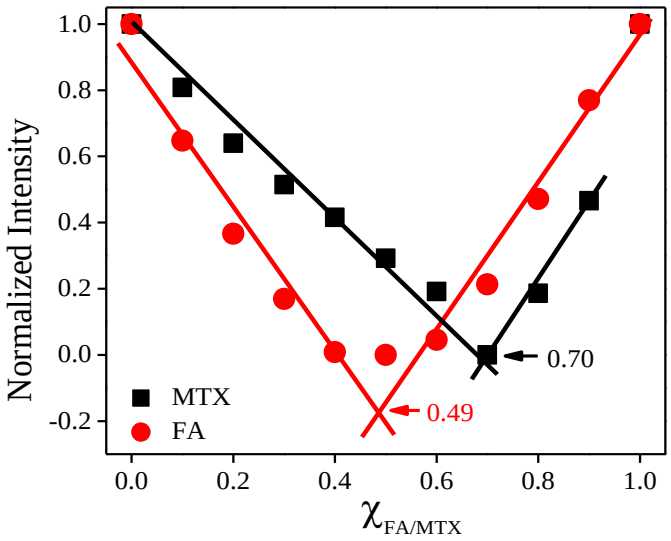

Figure S7. The Job's plot for HSA − drug complex at pH 7.4 and 298 K.

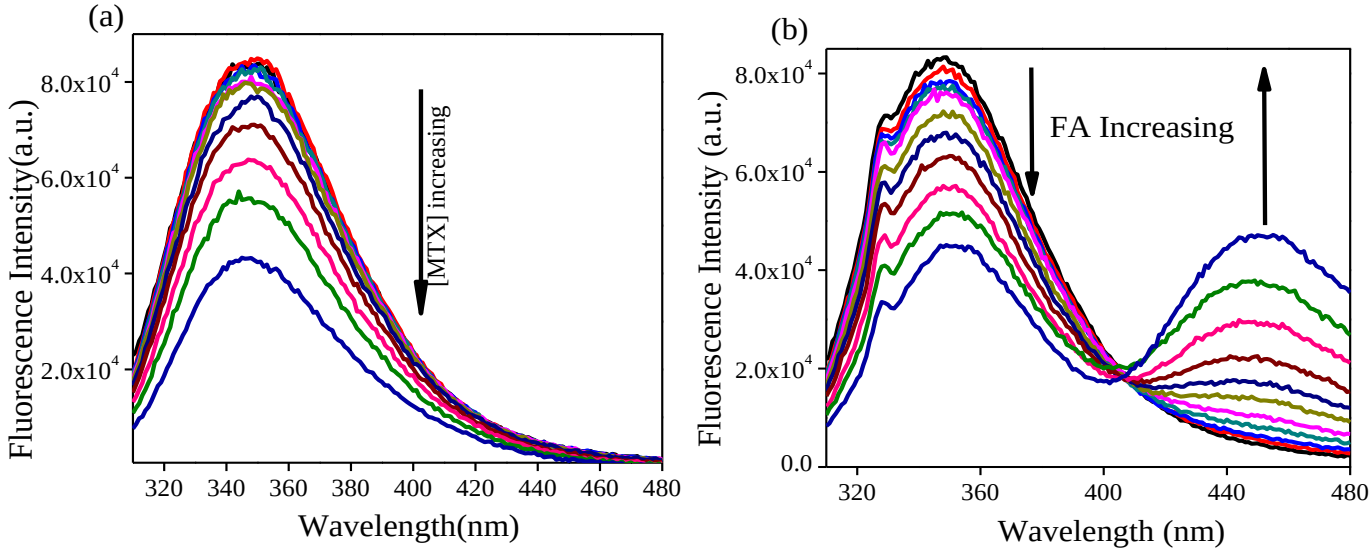

Figure S8. Fluorescence emission spectra (λ_{ex} 295nm) of HSA (2 μM) in the presence of different concentration of (a) MTX and (b) F A (from 0 to 30 μM) at 298K.

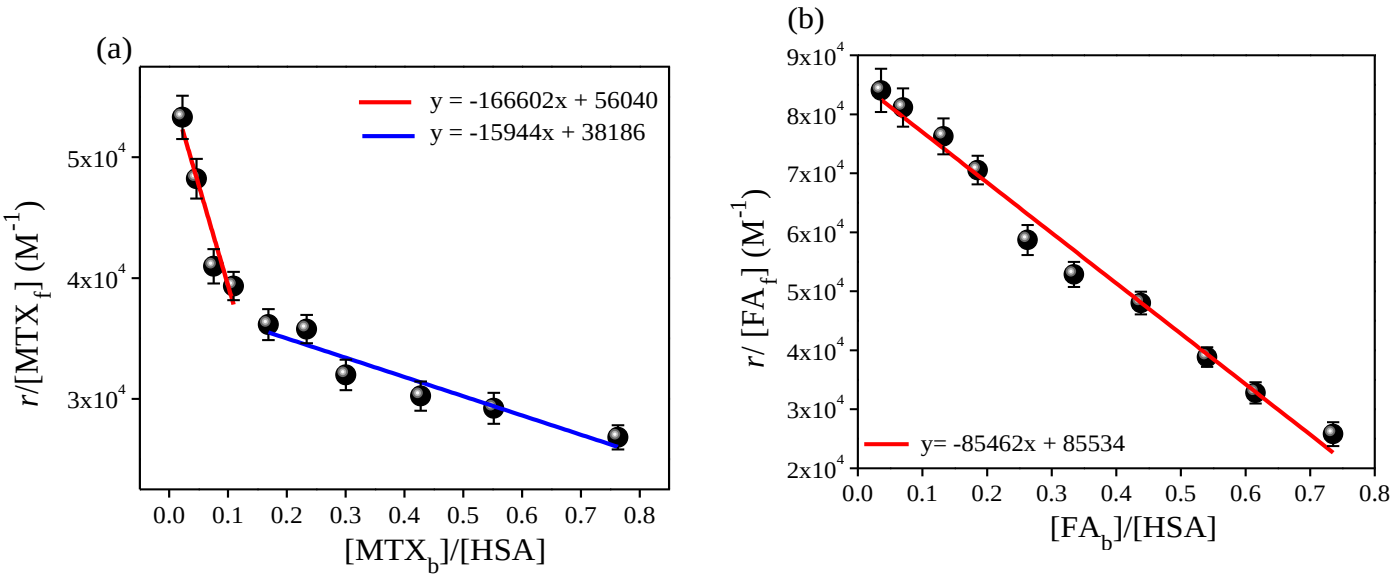

Figure S9. Scatchard plot (λ_{ex} = 280 nm) of the binding of (a) MTX and (b) FA with HSA for two component system at 298K.

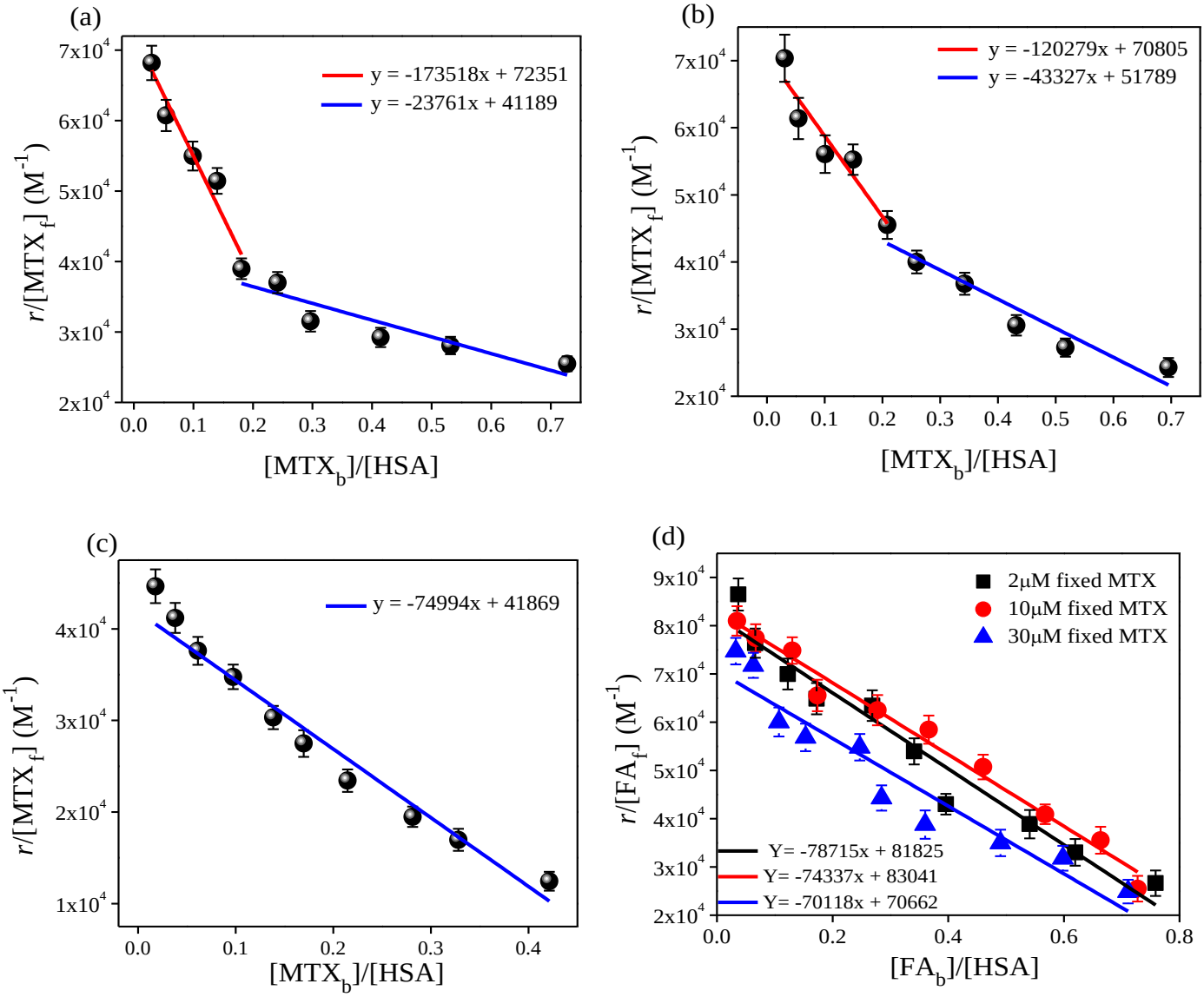

Figure S10. Scatchard plot of the binding (λ_{ex} = 295 nm) for two component system at 298K of MTX with fixed concentration of FA (a) 2 μM (b) 10 μM and (c) 30 μM. Also (d) Scatchard plot of the binding FA with fixed concentration of MTX (2 μM 10 μM and 30 μM).

Docking Analysis and Possible Mode of Interaction

We investigate the possible locations of these two drugs molecule with the help of docking analysis. The geometry of MTX and FA has been first optimized by PM3 prescription using Gaussian 03 and the resultant geometries have been read in AutoDock 4.2 software in compatible file format, from which the required file is generated in AutoDock 4.2.[3] The grid size is set to 60, 60, and 60 along the x-, y-, and z-axis with 0.5 Å grid spacing; i.e., to recognize the drugs within the binding pockets of HSA. The lowest binding energy conformer has been searched out of 80 different conformers for each docking simulation, and the resultant one is used for further analysis. In this case, blind docking of MTX and FA have been performed into the 3D Crystal structure of HSA and it has been found that MTX majorly binds in the two sites, whereas preferable site for FA is one, as the experimental result suggest. To get the competitive binding account, we performed docking over one pre-exists drug molecule. Now combining the result of the experimental findings and docking simulations have been described, making the following points.

(a) Both of MTX molecules are found to bind nearer to the Trp214 (~ 4-10Å) and far apart from Tyr150, indicate that the binding interaction is majorly characterized by the quenching of typical Trp fluorescence. From the surrounding amino acid residue, we can determine preferable binding pocket of MTX in the HSA (Lys195, Gln196, Lys199, Trp214, Gln221, Arg218, Arg222, Leu238, His242, Ala291, Glu292, Val343, His440, Lys444, Pro447, Lys448, Asp451 for site I and Phe206, Arg209, Ala210, Ala213, Trp214, Asp324, Leu327, Gly328, Leu331, Leu347, Ala350, Lys351, Leu481, Val482 for site II) and it is the subdomain IIA and IIIA (see the Figure S11). Minimum energy docked pose of FA is displayed in Figure S12, and adjacent protein residues (within 6.0 Å) surrounding the protein-bound drug molecule (Tyr150, Lys195, Lys199, Trp214, Arg218, Leu219, His242, Arg257, Ala291, Glu292, Asn295, Lys444, Pro447, Lys448) reveal that FA prefers to bind in subdomain IIA.

(b) Positively charged amino acid residues, such as Lys, Arg, and His, around the docked ligands, are responsible for electrostatic interaction in subdomain IIA and they mostly prefer the anionic form of drugs. The docked poses also indicate that the negatively charged amino acid residue (Asp 451) is largely

separated from the drugs molecules (although MTX and Asp distance is around 4Å, this type of interaction shows minimal effect due to presence of concentrated positive charge), and hence it shows little contribution on the pocket charge alterations.

(c) In competitive binding, MTX favors binding in the second site without alteration of the location of the drug (see the Figure S13). As this site possess less charged amino acid residue, the π-π interactions are the presumably major binding factor here.

(d) The change in SASA value also displayed the significant involvement of side chain amino acid reduces shown in Table S3. This table suggests that ΔSASA value of positively charged and polar uncharged side chain residues is significantly altered for docking of the molecule in first binding site. At the second binding site, the ΔSASA value of hydrophobic residues is predominantly changed, although the noticeable change in ΔSASA value of Arg209 and Lys351 residues also implies some involvement of the positive charge in this pocket.

Therefore, the molecular docking studies have been found to corroborate the conclusions from the experimental results, infers that FA prefers to bind in subdomain IIA (first binding site), i.e., by the conversion of FA to folate, and due to predominant dual binding site of MTX, prefers to reside in subdomain IIIA (second binding site). When FA is present in the first site, the π-π interactions as the major binding force of MTX with surrounding amino acid residues.

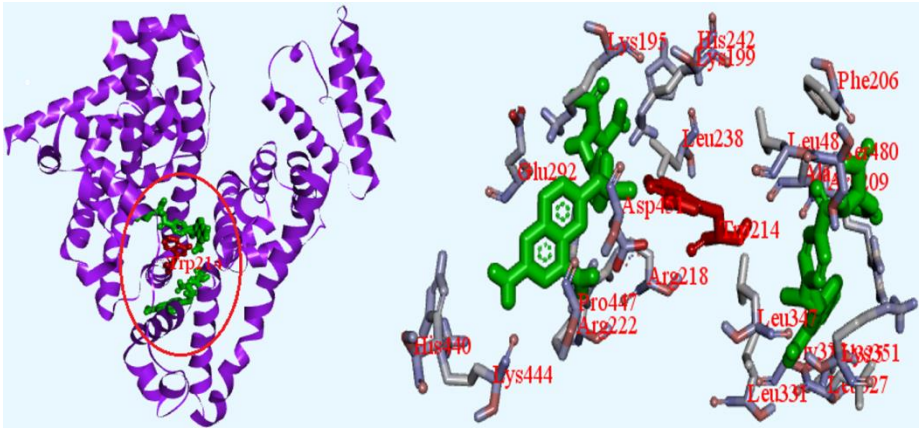

Figure S11. Stereo view of the docked conformation of two MTX around the Trp214 of the HSA and adjacent figure displays the adjacent protein residues (within 6.0 Å) of the MTX, where the location of these two MTX are concentrated in the site I and site II, respectively.

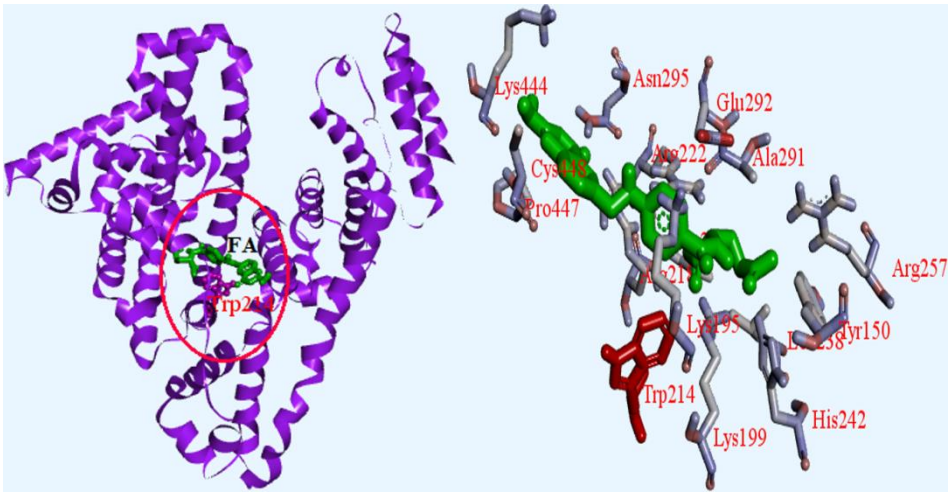

Figure S12. Stereo view of the docked conformation of one FA around the Trp214 of the HSA and adjacent figure displays the adjacent protein residues (within 6.0 Å) of the FA, where location of this one FA is concentrated in the site I.

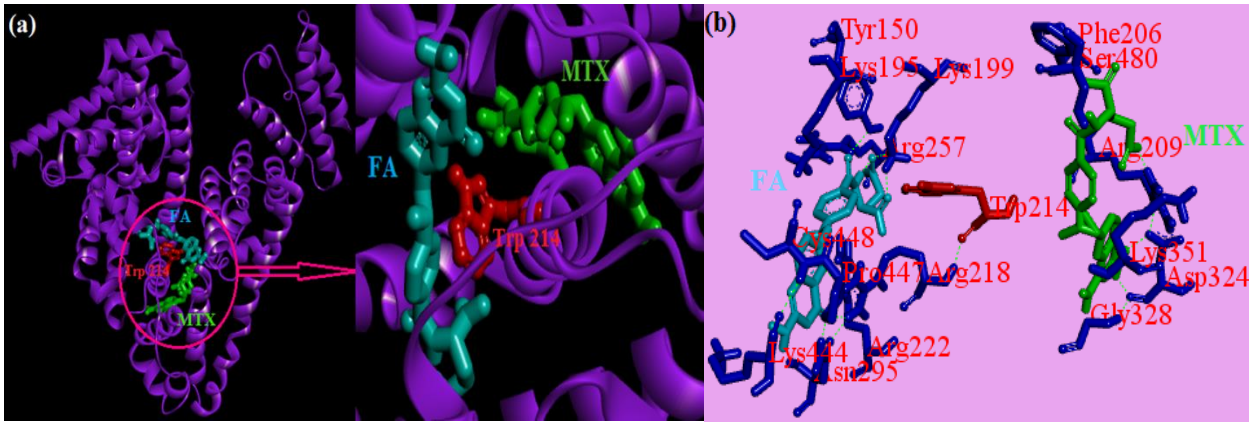

Figure S13. (a) Stereo view of the docked conformation of the MTX and FA around the Trp214 of the HSA. (b) Displays the adjacent protein residues (within 6.0 Å) of the drugs, where location of FA and MTX are regarded as the site I and site II, respectively.

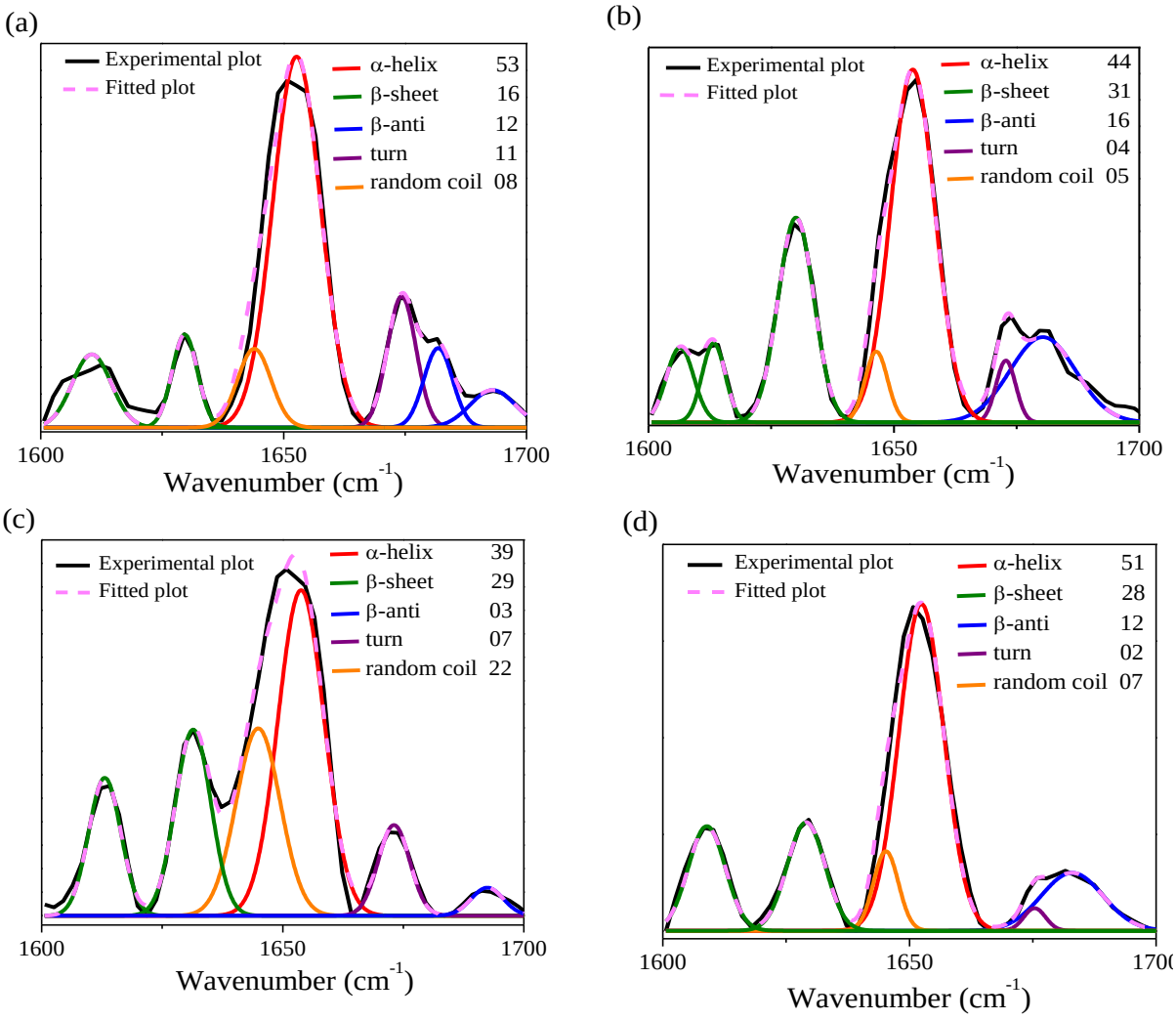

Figure S14. Curve-fitted inverted second-derivative amide I spectrum for the (a) free HSA (250 μM) and HSA in presence of (b) FA (500 μM), (c) MTX (500 μM) and (d) MTX (250 μM) and FA (250 μM) both.

Table S1. Fluorescence Lifetimes, Quantum Yield, and Radiative and Nonradiative Decay Constant of MTX and FA in Absence or Presence of HSA at 298K.

System	[HSA] (μM)	τ_1 (a_1) (ns)	τ_2 (a_2) (ns)	τ_3 (a_3) (ns)	τ_{avg} (ns)	Quantum yield (Φ)	$\kappa_r \times 10^6$ (s^{-1})	$\kappa_{nr} \times 10^8$ (s^{-1})
MTX	0	--	2.27 (0.81)	6.95 (0.19)	3.16	0.0018	0.57	3.16
	2	0.46 (0.13)	2.45 (0.69)	7.19 (0.18)	3.05	0.0018	0.57	3.27
	5	0.49 (0.15)	2.41 (0.66)	7.07 (0.19)	3.01	0.0017	0.57	3.32
	10	0.43 (0.21)	2.41 (0.60)	7.05 (0.19)	2.88	0.0017	0.59	3.47
	20	0.35 (0.27)	2.29 (0.54)	6.97 (0.19)	2.66	0.0017	0.63	3.75
	30	0.31 (0.36)	2.29 (0.47)	7.08 (0.17)	2.39	0.0017	0.70	4.18
	50	0.38 (0.42)	2.36 (0.41)	7.23 (0.17)	2.36	0.0016	0.70	4.23
	70	0.41 (0.47)	2.39 (0.37)	7.23 (0.16)	2.24	0.0016	0.73	4.46
	100	0.37 (0.50)	2.25 (0.34)	7.16 (0.16)	2.10	0.0016	0.80	4.75
FA	0	0.53 (0.77)	2.85 (0.13)	7.39 (0.10)	1.52	0.0094	6.21	6.52
	2	0.51 (0.78)	2.92 (0.12)	7.43 (0.10)	1.49	0.0074	4.73	6.66
	5	0.46 (0.77)	2.77 (0.13)	7.45 (0.10)	1.46	0.0056	3.84	6.81
	10	0.38 (0.76)	2.36 (0.15)	7.48 (0.09)	1.31	0.0045	3.46	7.59
	20	0.28 (0.70)	1.91 (0.21)	7.35 (0.09)	1.26	0.0038	3.04	7.90
	30	0.29 (0.72)	2.06 (0.20)	7.80 (0.08)	1.25	0.0034	2.74	7.97
	50	0.30 (0.75)	2.04 (0.16)	7.34 (0.09)	1.21	0.0029	2.36	8.24
	70	0.29 (0.74)	1.96 (0.18)	7.39 (0.08)	1.16	0.0025	2.15	8.60
	100	0.26 (0.76)	1.92 (0.16)	7.28 (0.08)	1.09	0.0024	2.23	9.15

Table S2. Rotational Correlation Time (θ_r) of MTX and FA in Absence or Presence of HSA at 298K.

System	[HSA] (μM)	θ_1 (a_1) (ns)	θ_2 (a_2) (ns)	θ_r (ns)	χ^2
MTX	0	0.20(1.00)	--	0.20	1.03
	20	0.38(1.00)	--	0.38	0.92
	100	1.34(1.00)	--	1.34	0.90
FA	0	0.11(1.00)	--	0.11	1.16
	20	0.26(0.63)	3.80(0.37)	1.57	1.02
	100	0.46(0.63)	5.39(0.37)	2.28	0.85

Table S3. Change in accessible surface area (ΔSASA) in $Å^2$ of interacting residues of HSA (uncomplexed) and their complex with MTX, FA and MTX-FA. (I represent the site I or subdomain IIA and II represent the site II or subdomain IIIA)

MTX-HSA				**FA-HSA**		**FA-MTX-HSA**			
I		**II**		**I**		**I**		**II**	
Lys195	61.166	**Phe206**	24.153	**Tyr150**	2.438	**Tyr150**	10.28	**Phe206**	23.146
Gln196	6.82	**Arg209**	54.613	**Lys195**	38.537	**Lys195**	38.537	**Arg209**	49.646
Lys199	29.108	**Ala210**	11.07	**Lys199**	27.095	**Lys199**	27.095	**Trp214**	19.121
Trp214	33.065	**Ala213**	26.668	**Trp214**	19.121	**Trp214**	19.121	**Leu327**	13.587
Gln221	0.472	**Trp214**	33.065	**Arg218**	40.75	**Arg218**	40.75	**Asp324**	14.672
Arg218	31.934	**Asp324**	14.201	**Leu219**	6.038	**Leu238**	24.656	**Leu331**	13.587
Arg222	23.38	**Leu327**	14.089	**His242**	0	**His242**	0	**Gly328**	8.051
Leu238	17.108	**Gly328**	8.051	**Arg257**	6.388	**Arg257**	6.388	**Val343**	0
His242	0	**Leu331**	7.548	**Ala291**	15.096	**Glu292**	15.096	**Leu347**	8.051
Ala291	16.102	**Leu347**	8.051	**Glu292**	6.477	**Asn295**	6.447	**Ala350**	13.082
Glu292	7.1	**Ala350**	13.082	**Asn295**	19.922	**Lys444**	19.992	**Lys351**	29.607
Val343	2.516	**Lys351**	25.646	**Lys444**	14.399	**Pro447**	17.399	**Ser480**	17.971
His440	17.415	**Leu481**	6.038	**Pro447**	17.611	**Lys448**	7.883	**Leu481**	6.038
Lys444	8.361	**Val482**	21.134	**Lys448**	7.883			**Val482**	21.134
Pro447	13.585								
Lys448	14.088								
Asp451	23.801								

Table S4. α-Helix contents of HSA at pH 7.4 (at 298 K) in absence and presence of MTX and FA.

System	[Drug] (μM)	α-helix of HSA (%)
MTX	0	52.71
	5	52.19
	10	51.76
	20	51.40
	50	50.83
FA	0	52.71
	5	52.58
	10	52.43
	20	52.26
	50	52.19

- **REFERENCES**

(1) Lakowicz, J. R. *Principles of Fluorescence Spectroscopy*, 3rd ed.; Springer: New York, 2006.

(2) Li, G. F.; Magana, D.; Dyer, R. B. Photoinduced Electron Transfer in Folic Acid Investigated by Ultrafast Infrared Spectroscopy. *J. Phys. Chem. B* **2012**, *116*, 3467-3475.

(3) Morris, G. M.; Goodsell, D. S.; Halliday, R. S.; Huey, R.; Hart, W. E.; Belew, R. K.; Olson, A. J. Automated Docking Using a Lamarckian Genetic Algorithm and an Empirical Binding Free Energy Function. *J. Comput. Chem.* **1998**, *19*, 1639-1662.